Geometrical model of multiparticle production in hadron-hadron collisions

T. T. Chou
Department of Physics, University of Georgia, Athens, Georgia 30602

Chen Ning Yang
Institute for Theoretical Physics, State University of New York, Stony Brook, New York 11794
(Received 6 May 1985)

A recently introduced concept of partition temperature in the geometrical model of multiparticle production processes in high-energy hadron-hadron collisions is presented in detail. Extrapolations to $\sqrt{s}=53$ GeV, 2 TeV, and 40 TeV are made.

I. DESCRIPTION OF THE GEOMETRICAL MODEL FOR MULTIPARTICLE PRODUCTION PROCESSES

A. Separation of stochastic from nonstochastic aspects of collision

Recently, new ideas have been introduced[1-3] to the geometrical model for multiparticle production processes in hadron-hadron collisions. The most important feature of the new development is the separation of the stochastic and nonstochastic [i.e., approximate Koba-Nielsen-Olesen (KNO) scaling[4]] aspects of the collision which led to the concept of partition temperature T_p and the single-particle momentum distribution discussed in Ref. 3.

B. Details of model

We shall now give a detailed description of the geometrical model for inelastic hadron-hadron collisions. Justification of the model and further consideration will be given in subsequent sections.

The geometrical model is summarized in Figs. 1(a)—1(c) for elastic, double-diffraction dissociation, and nondiffractive processes. We omit "single-diffraction dissociation" processes which are usually defined as those resulting in a few particles on one side and many on the other. They are omitted because we believe such processes will become insignificant at very high energies. More about this later.

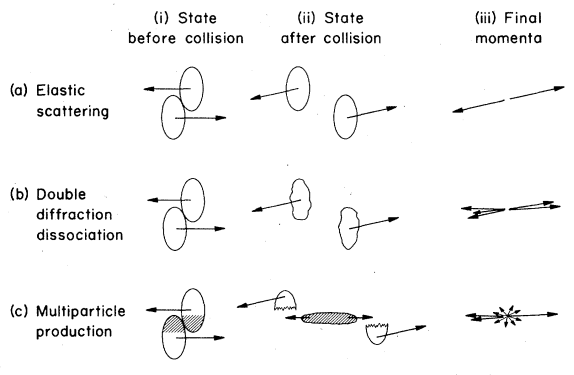

FIG. 1. Schematic diagrams depicting (a) elastic-scattering, (b) double-diffraction-dissociation, and (c) multiparticle-production processes.

For elastic processes illustrated in Fig. 1(a), the two hadrons "pass through" each other[1] with a surviving amplitude $S(b)$=the S matrix at impact parameter b. According to the Huygens principle, the elastic-scattering amplitude is the Fourier transform of $1-S(b)$. More precisely, we obtain[1] the elastic-scattering cross section

$$d\sigma/dt=\pi|\langle 1-S\rangle|^2, \tag{1}$$

where

$$\langle 1-S\rangle=(2\pi)^{-1}\int\int[1-S(b)]\exp(i\mathbf{k}\cdot\mathbf{b})d^2b \tag{2}$$

and

$$-t=\text{momentum-transfer squared in center-of-momentum system}=k^2. \tag{3}$$

For the double-diffraction-dissociation[5] processes illustrated in Fig. 1(b), the hadrons pass through and possibly excite each other, with the excited states later fragmenting into fast hadrons with small transverse momenta.

We shall now describe the last type of collisions: the nondiffractive process illustrated in Fig. 1(c). For each impact parameter b, a certain part of each of the incoming hadrons proceeds with (essentially) its original velocity, resulting in the unshaded parts in Fig. 1(c)(ii), which carry the energies $E_0(1-h_F)$ and $E_0(1-h_B)$ where E_0 is the energy of each of the incoming hadrons, and h_F and h_B are fractions of forward and backward energies that reside in the shaded part. The unshaded parts later fragment into leading particles. The shaded parts exchange longitudinal and transverse momenta, resulting in the central region in Fig. 1(c)(ii). The forward moving part of this long region then has its energy partitioned into that of many particles moving in the forward direction. Similarly for the backward moving part.

C. Partition temperature T_p

In this model, for pp and $\bar{p}p$ collisions at high energies, $h_F\simeq h_B$ $(=h)$, and the multiplicities of particles on the

TABLE I. Parameters for multiparticle production processes at $\sqrt{s}=540$ GeV. $n_{\rm obs}$, which labels different charge-multiplicity ranges, is different from the true charge multiplicity by a factor of approximately 1.25 due to experimental corrections. For a given charge multiplicity, the shape of the experimental $dn/d\eta$ curve is well fitted by Eq. (4) of Ref. 3 for one value of T_p. The parameter h and normalization constant K are both determined from the curves themselves. The average values for the impact parameter are rough estimates based on a procedure outlined in Ref. 10. The total longitudinal momentum transfer is estimated by summing $(e-p_{\parallel})$ over all central-region particles (charged and neutral) using Eq. (4) of Ref. 3. Contributions to longitudinal momentum transfer from particles in the fragmentation region are negligible.

$n_{\rm obs}$	Partition temperature T_p (GeV)	Normalization constant K (GeV^{-2})	$n_{\rm cal}$	KNO variable $z=n_{\rm cal}/\bar{n}$	Energy fraction in central region $=h$	Average energy per particle in central region (GeV)	Average impact parameter b (fm) (approximate)	Longitudinal momentum transfer (GeV)
≥ 71	4.4	83	99	3.4	0.45	1.6	0.02	9.2
51—70	6.3	54	73	2.5	0.42	2.1	0.1	6.4
41—50	6.8	40	55	1.9	0.33	2.2	0.3	4.7
31—40	8.8	29	44	1.5	0.32	2.6	0.6	3.6
21—30	14	20	33	1.1	0.31	3.4	0.9	2.5
11—20	24	11	21	0.73	0.26	4.4	1.3	1.5
≤ 10	180	4.8	11	0.37	0.20	6.6	1.8	0.67

two sides are approximately equal,

$$n_F=n_F^{\rm ch}\simeq n_B^{\rm ch}=n_B,\quad n_F^{\rm neutral}\simeq n_B^{\rm neutral}\ .$$

More precisely,

$$n_F^{\rm ch}=n_B^{\rm ch}+O((n_B^{\rm ch})^{1/2}),\ \text{etc}\ .$$

The partition of energy into outgoing particles on each side is a stochastic process governed by (i) the requirement that the total energy of all outgoing particles on each side be E_0h, (ii) the transverse-momentum cutoff factor $g(p_\perp)$, (iii) the Bloch-Nordsieck factor d^3p/E, and (iv) correlation effects between particles. The simplest stochastic distribution[3] for a single particle on each side, not taking into account effect (iv), is

$$dn=dn^{\rm ch}=K(d^3p/E)g(p_\perp)\exp(-E/T_p)\ , \tag{4}$$

where T_p is the "partition temperature."

For 540-GeV $\bar{p}p$ collisions at the CERN Collider, for different impact parameters b, the values of h, T_p, and the total charge multiplicity n, etc., were given in Ref. 3 and are reproduced in Table I.

D. Inelasticity

We remark that the leading particles take away a fraction $(1-h)$ of the total energy, and this fraction according to Table I is $\geq 50\%$ *for all collisions* at the CERN Collider. Averaged over all nondiffractive collisions this fraction is $1-\bar{h}=72\%$. The remaining fraction $\bar{h}=28\%$ of the incoming energy represents the average energy that goes into the multiparticle production process [shaded part of Fig. 1(c)(ii)]. It is what has been called "inelasticity" by cosmic-ray[6] physicists. In recent years, Basile *et al.*,[7] have emphasized the importance of the leading particle effect, which is related to the fact that h is less than 100%.

Experimental estimation of the value of h for each collision has always in the past come up with an ambiguity because it is not clear which of the fast particles (in the c.m. system) should be included in the "central region" (shaded part) and which in the fragmentation region (unshaded part). Since a fast particle contributes a large chunk of energy, this ambiguity has made it very difficult to give any accurate evaluation of the fraction h. With the introduction of the partition temperature T_p and Eq. (4) this difficulty disappears: Take the 540-GeV $\bar{p}p$ collision discussed in detail in Ref. 3. For each total multiplicity in Table I and Fig. 4, T_p is determined from the *experimental* η distribution, mainly for low values of η, say $0<\eta<4$. Having determined T_p, Eq. (4) then allows for a *calculation of the small tail* of the curve for $\eta>5$. The magnitude of this tail then makes possible an accurate evaluation of the contribution to h from the $\eta>4$ part. Thus this contribution is evaluated not from $\eta>4$ data which are inaccurate, but from lower-η data together with Eq. (4).

E. Increase of T_p with impact parameter b

In remark (a) of Ref. 3, the increase of T_p with b, seen in Table I, is given a natural qualitative physical reason based on the geometrical picture.

F. Longitudinal momentum transfer

The value of the total longitudinal momentum transfer is listed in the last column of Table I. We see that its value is very small for low-multiplicity events. Even for the high-multiplicity events, its value is only 9.2 GeV $=3.4\%$ of the incoming momentum. This presents a picture of small-impact-parameter collisions which is not what one may at first anticipate: For such collisions, the incoming hadrons are quite opaque to each other. The survival amplitude[8]

$$S(b=0)=\exp[-\Omega(0)]$$

is only ~ 0.19, so that only $\sim 4\%$ of such collisions are elastic. The point is that for the remaining 96% of such

collisions, the result is very far from a "bang," (i.e., an amalgamation of the two hadrons in one region of space, as in the early Fermi picture[9]). Instead, the longitudinal momentum exchange between the two sides is only $\sim 3\%$. (Of course, there is bound to be a process in which thousands of particles are emitted in the c.m. system, all nearly at rest. Such processes would involve a large longitudinal momentum transfer of ~ 270 GeV, and would require $h=1$. But that would clearly have *extremely* small cross sections.)

The smallness of the longitudinal momentum transfer, even for processes involving the production of many particles, indicates what we may call the *persistence of longitudinal momentum* in very-high-energy hadron-hadron collisions. This is a dominating characteristic: For the 540-GeV $\bar{p}p$ Collider, elastic and double-diffraction-dissociation events [Figs. 1(a) and 1(b)] involve longitudinal momentum transfers of the order of at most a few dozen MeV's, while the nondiffractive events [Fig. 1(c)] involve longitudinal momentum transfers of the order of a few GeV's, not more. Larger longitudinal momentum transfers are *extremely* rare.

II. JUSTIFICATION OF MODEL

A. Large range of total angular momentum

For $\bar{p}p$ collision at 540 GeV, the total angular momentum J of the collision ranges from 0 (for $b=0$) to $2000\hbar$ (for $b=1.5$ fm). It is clear that a collision at $J=0$ cannot possibly resemble one at $J=2000\hbar$. For higher incoming energy, the range of J would further increase. We believe this is the fundamental reason[10] for the wide fluctuation in multiplicity (KNO scaling or approximate KNO scaling) in high-energy hadron-hadron collisions.

Accepting this view it is natural to assume that, for a single b, the fluctuation should not be large. We believe this is in agreement[2] with experimental data,[11] a subject which we shall now discuss.

The UA5 Collaboration has studied[11] the probability distribution $P(n_F,n_B)$ of events with n_F,n_B, respectively, denoting the forward and backward charge multiplicities. Their result is reproduced here in Fig. 2. In Ref. 2 we have analyzed this diagram and found that along each fixed $n=n_F+n_B$ line, the probability distribution is well fitted by a binomial distribution. We call such distributions "stochastic," which according to Webster's dictionary means "of, pertaining to, or arising from chance." *Thus along the n_F+n_B direction, the distribution is non-stochastic due to fluctuations in b, and along the n_F-n_B direction the distribution is stochastic.*

Extrapolating these conclusions to very high energies and very-high-average multiplicities $\bar{n}$, we believe[2,3] the probability distribution $P(n_F,n_B)$ plotted against the scaled variables $n_F/\bar{n},n_B/\bar{n}$ would shrink from a fat cigar-shaped region to a thin cigar to essentially a line along which

$$n_F=n_B+O(n^{1/2}), \tag{5}$$

as illustrated in Fig. 3.

We emphasize here that a collision with forward and backward multiplicities n_F and n_B populating region (5) will exhibit a dramatic correlation. Take a case where $\bar{n}=10\,000$, say. Then n_F fluctuates widely, say, from 2000 to 15 000. But for each n_F,

$$n_B\sim n_F\pm\sqrt{10\,000}=n_F\pm 100$$

fluctuates very little.

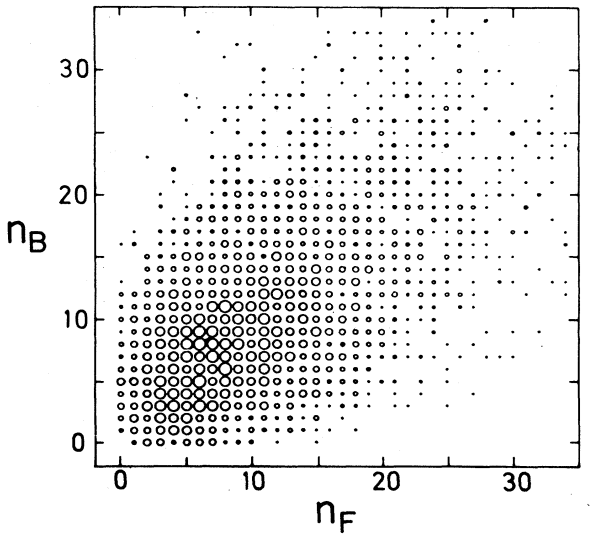

FIG. 2. Scatter plot of backward and forward multiplicities n_B and n_F for the η intervals $4>\eta_F>0$ and $0>\eta_B>-4$ at 540 GeV. For each value of (n_B,n_F) the area of the circle is proportional to the number of events. (Reproduced from Ref. 11.)

B. Stochastic partition at a single impact parameter b

The narrow line in Fig. 3 could be considered as a superposition of small circles as shown, each of which represents a stochastic fluctuation. Thus we arrive at the suggestion[2,3] that for very-high-energy collisions, for each impact parameter b, there are only stochastic fluctuations.

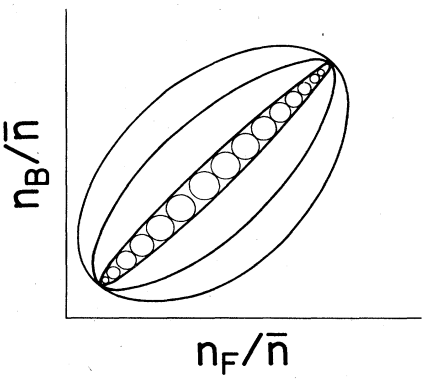

FIG. 3. Schematic diagram showing scaled forward-backward multiplicity distribution $P(n_F/\bar{n},n_B/\bar{n})$. Each contour line represents, say, 25% of the maximum value for P at a given energy. The contour lines shrink to the form of a thin cigar at very high energies.

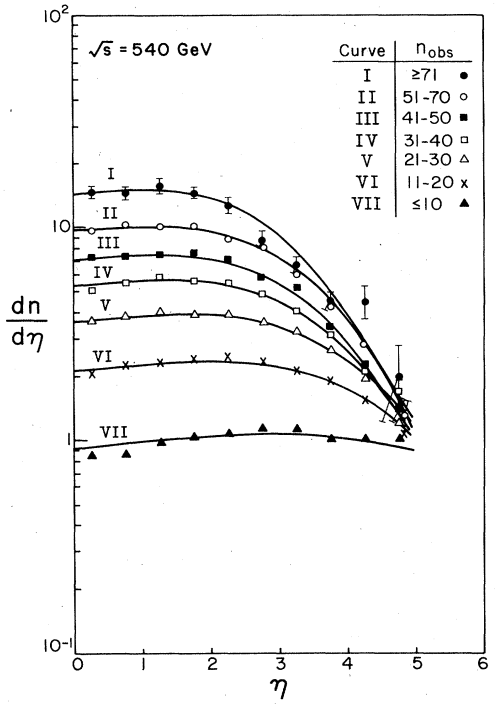

FIG. 4. $dn/d\eta$ versus η at $\sqrt{s}=540$ GeV. Data points are taken from UA5 experiments, Ref. 12.

It is the mixing of different b's that result in the observed larger nonstochastic (approximately KNO) fluctuation of the multiplicity.

Developing this view we were led[3] to the idea that, since for a fixed b the particle number distribution on each side is stochastic, for a fixed b the energy partition on each side must also be stochastic. This idea results in the concept of partition temperature T_p which governs the stochastic partition of energy on each side. A consequence of all these is Eq. (4) for the single-particle momentum distribution.

C. Comparison with experimental angular distribution

In Ref. 3, the angular distribution for each b (i.e., total multiplicity) is evaluated from Eq. (4) and compared with the experimental results of UA5 for $\bar{p}p$ collisions at 540 GeV total energy. The agreement is excellent. Furthermore, there are no adjustable parameters in this comparison, which is reproduced here as Fig. 4.

D. Decrease of single diffraction events

It is obvious from Fig. 3 that for higher and higher energies, strongly forward-backward asymmetrical events will become progressively unimportant. In particular, the fraction of single-diffraction events, events for which there are only a few diffractive fast particles on one side, while there are many particles emitted on the other, will become very rare. This is consistent with the UA5 result[12] indicating that the fraction of single-diffraction events rapidly decreases with increasing energy.

III. EXTRAPOLATION TO HIGHER AND LOWER ENERGIES

We made extrapolations of the angular distribution to $\sqrt{s}=53$ GeV (CERN ISR energy), 2 TeV (Fermilab Tevatron), and 40 TeV [Superconducting Super Collider (SSC)]. The assumptions made in these computations are as follows: (i) The $p_\perp$ cutoff factor $g(p_\perp)$ is taken to be

$$g(p_\perp)=\exp(-\alpha p_\perp)\ , \tag{6}$$

where we take[12,13]

$$\begin{aligned}&\alpha=5.8\ (\mathrm{GeV}/c)^{-1}\ \text{ for } \sqrt{s}=53\ \mathrm{GeV}\ ,\\ &\alpha=5.0\ (\mathrm{GeV}/c)^{-1}\ \text{ for } \sqrt{s}=2\ \mathrm{TeV}\ ,\\ &\alpha=4.4\ (\mathrm{GeV}/c)^{-1}\ \text{ for } \sqrt{s}=40\ \mathrm{TeV}\ .\end{aligned} \tag{7}$$

(ii) The parameter h is taken to be a function only of the KNO variable $z=n/\bar{n}$. (iii) The value of $\bar{n}_{\mathrm{ch}}$ for these energies are taken to be 13, 41, and 78, respectively.[14] The results are presented in Fig. 5 and Table II. For previous extrapolation, see Ref. 13.

Is this method of extrapolation reasonable? In particular, with this method, for fixed central energy $2E_0h$, but for increasing E_0, the multiplicity n will decrease. (For

TABLE II. Parameters for single-particle distribution at ISR, Tevatron, and SSC energies. The relation between α and $\langle p_\perp\rangle$ is given by $\alpha=2\langle p_\perp\rangle^{-1}$. n is the total charge multiplicity. The normalization constant K is in GeV^{-2} and partition temperature T_p in GeV.

		$\sqrt{s}=53$ GeV ($\alpha=5.8$ GeV^{-1})			$\sqrt{s}=2$ TeV ($\alpha=5.0$ GeV^{-1})			$\sqrt{s}=40$ TeV ($\alpha=4.4$ GeV^{-1})		
z	$h(z)$	n	K	T_p	n	K	T_p	n	K	T_p
3.4	0.45	44	350	0.25	140	71	17	270	62	300
2.5	0.42	33	140	0.43	100	48	23	200	44	400
1.9	0.33	25	91	0.49	78	36	25	150	33	420
1.5	0.32	20	53	0.70	62	27	31	120	26	520
1.2	0.31	15	27	1.2	47	19	43	89	18	700
0.73	0.26	10	13	2.0	30	11	61	57	11	950
0.37	0.20	5	3.9	32	15	5.1	130	29	5.3	1700

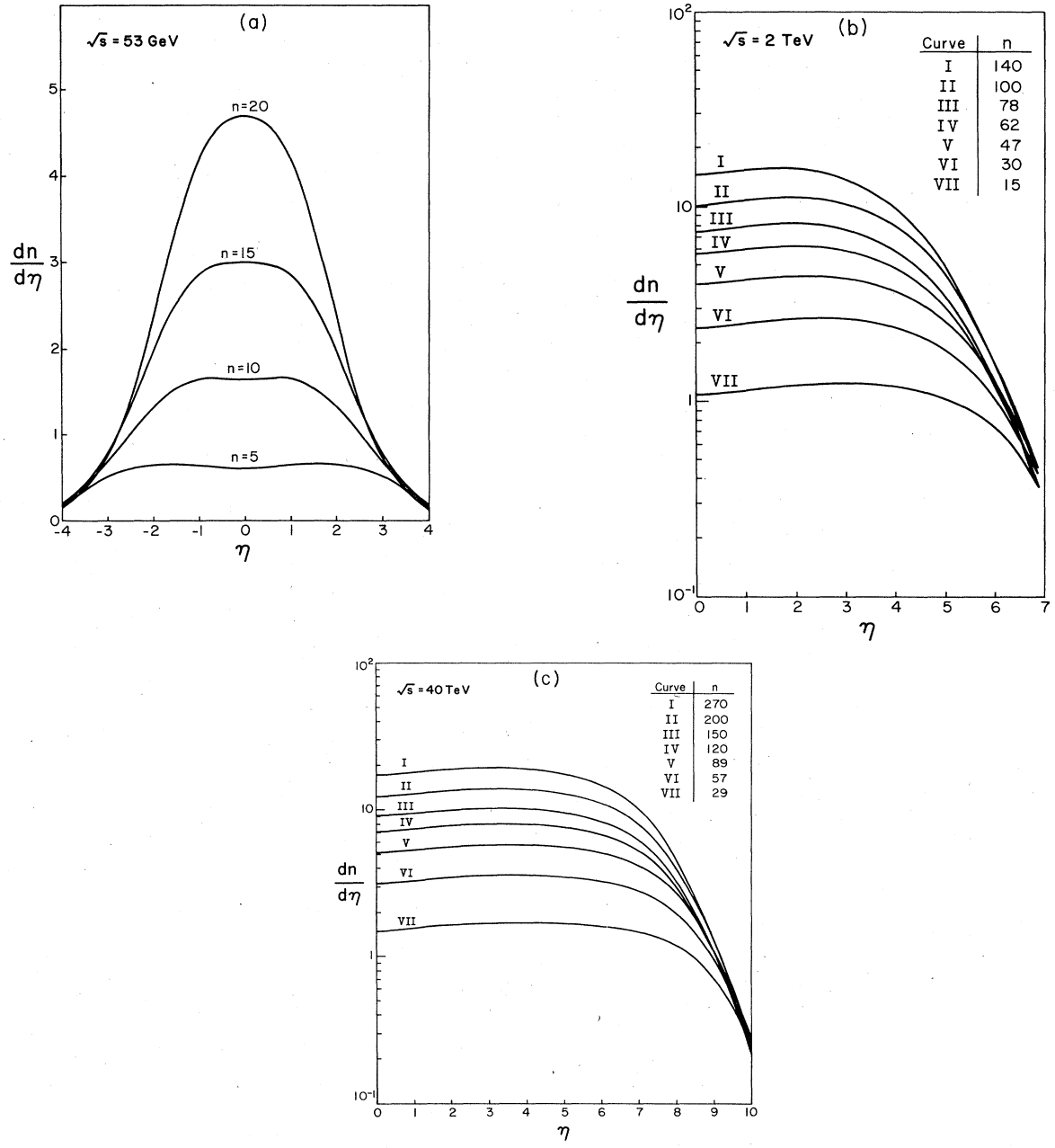

FIG. 5. Calculated $dn/d\eta$ versus η at (a) $\sqrt{s}=53$ GeV, (b) $\sqrt{s}=2$ TeV, and (c) $\sqrt{s}=40$ TeV.

example, take the case $E_0=270$ GeV, $h=0.42$ for which $n=73$ and $z=n/\bar{n}=2.5$ according to Table I. Consider next the case $E_0'=540$ GeV, $h'=0.21$ which shares the same value of $E_0'h'=113$ GeV$=E_0$h. $h'=0.21$ gives $z'=n'/\bar{n}'\simeq 0.4$. We estimate $\bar{n}'\simeq 35$. Thus $n'\simeq 14$ which is much smaller than $n=73$.) One may ask, for a given total central region energy $2E_0h$, why should there not be just a unique multiplicity n of emitted charged particles. We believe the answer to this question resides in the fact that besides the total central-region energy $2E_0h$, there is an additional important parameter, the total angular momentum of the central region. The multiplicity should depend on both of these variables, and for given $2E_0h$ could vary with E_0.

It is perhaps reasonable to expect $h(z,E_0)$ and the dimensionless parameter $f(z,E_0)=T_p/E_0$ to depend on E_0 slowly, for any fixed z. For example,

$$h(z,E_0)=h_0(z)+h_1(z)\ln(E_0/1\text{ GeV})\,, \tag{8}$$

$$f(z,E_0)=f_0(z)+f_1(z)\ln(E_0/1\text{ GeV})\,, \tag{9}$$

where

$$z=n/\bar{n}\,.$$

Data with the Fermilab Collider in the next few years will allow us to determine h_0, h_1, f_0, and f_1 in the $E_0=270-1000$ GeV range.

IV. REMARKS ON T_p

A. A thermodynamical model

In Ref. 3 the concept of partition temperature T_p was introduced by using the method of steepest descent. We shall shortcut this mathematical approach here and construct a thermodynamical model which will exhibit clearly the physical meaning of the parameter T_p and Eq. (4).

Consider a three-dimensional region in (x,y,z) space above the quarter plane $(x>0, y>0, z=0)$ and below the surface

$$z=\frac{y}{(m^2+x^2+y^2)^{1/2}}g(y)\ , \tag{10}$$

bounded on the sides by the planes $x=0$ and $y=0$. Consider a gas of noninteracting particles of mass $M=\infty$ moving in this region with a potential energy for each particle of

$$V=(m^2+x^2+y^2)^{1/2}\ . \tag{11}$$

A microcanonical ensemble for such a gas of N atoms at total energy $\mathscr{E}$ has a probability distribution of

$$\delta\left[\sum_1^N V_i-\mathscr{E}\right]\prod_1^N dx_i dy_i dz_i\ .$$

Integrating over all z_i gives

$$\delta\left[\sum(m^2+x_i^2+y_i^2)^{1/2}-\mathscr{E}\right]\times\prod_i\frac{y_i}{(m^2+x_i^2+y_i^2)^{1/2}}g(y_i)dx_i dy_i\ .$$

Replacing x_i by $(p_{||})_i$, y_i by $(p_\perp)_i$ this reduces to

$$\delta\left[\sum_i(m^2+p_{||i}^2+p_{\perp i}^2)^{1/2}-\mathscr{E}\right]\times\prod_i\left[\frac{p_\perp dp_\perp dp_{||}}{(m^2+p_{||}^2+p_\perp^2)^{1/2}}g(p_\perp)\right]_i\ .$$

Thus this microcanonical ensemble gives exactly the same distribution as Eq. (1) of Ref. 3. Similarly the canonical ensemble for this gas at temperature T_p gives exactly the same distribution as Eq. (2) of Ref. 3. The mathematical step that leads from Eq. (1) to Eq. (2) in Ref. 3 is then exactly the step familiar in physics that leads from the microcanonical to the canonical ensemble for the gas model.

B. Existence of T_p does not imply equilibrium

Although for the gas model the temperature T_p is an equilibrium concept, for the high-energy collision problem T_p is just a mathematical parameter that governs the partition of energy in the stochastic process at impact parameter b and neither requires nor implies equilibrium. This point is particularly clear if we concentrate on the factor d^3p/E in Eq. (1) of Ref. 3. We want to make the following observations. (a) Replacing d^3p/E with d^3p leads[3] to a single-particle distribution that totally disagrees with the angular distribution given by the UA5 group. (b) In any system in thermal equilibrium, such as for the black-body radiation, it is always the factor d^3p, not d^3p/E, that appears as the density of modes. Does the factor d^3p/E never occur for the problem of black-body radiation? The answer is yes, it does occur when we discuss certain nonequilibrium phenomena. For example, consider in a block of matter at a finite temperature a cavity which at $t=0$ is free of atoms and of all radiation. Immediately afterward, short- and long-wave radiation would begin to fill the cavity. Since the coupling of radiation with matter contains the factor d^3p/E, the long wavelength modes generally couple more strongly with matter and are filled faster. Thus in such a nonequilibrium situation, the factor d^3p/E does play a role. But in the long run, when equilibrium is established, *the strength of coupling is immaterial,* and only the mode density d^3p would play a role. (c) In a high-energy collision, there is not sufficient time to reach thermodynamical equilibrium in any part of the diagram of Fig. 1(c)(ii). The Bloch-Nordsieck factor then plays a role and gives rise to the factor d^3p/E.

V. ADDITIONAL REMARKS

(a) It is tempting to speculate that the observed π/K ratio in outgoing particles in the $\bar{p}p$ collider could be just the result of the effect of the masses m_π and m_K in Eq. (4), when the incoming energy is high enough. We are studying this question both qualitatively and quantitatively. Also studied is the question of two-particle correlation which was not taken into consideration in Ref. 3.

(b) Many of the concepts of the present paper have been discussed in various forms in the past by cosmic-ray and elementary-particle physicists. Some of these earlier discussions can be found in Ref. 15.

(c) We have extended the ideas of this paper to e^+e^- annihilations. See Ref. 16.

ACKNOWLEDGMENTS

This work was supported in part by the U.S. Department of Energy under Grant No. DE-FG09-84ER40160, and by the National Science Foundation under Grant No. PHY 81-09110 A01.

[1]T. T. Chou and C. N. Yang, Phys. Rev. **170**, 1591 (1968); Phys. Rev. D **22**, 610 (1980).
[2]T. T. Chou and Chen Ning Yang, Phys. Lett. **135B**, 175 (1984).
[3]T. T. Chou, Chen Ning Yang, and E. Yen, Phys. Rev. Lett. **54**, 510 (1985).
[4]Z. Koba, H. B. Nielsen, and P. Olesen, Nucl. Phys. **B40**, 317 (1972).
[5]M. L. Good and W. D. Walker, Phys. Rev. **120**, 1857 (1960).
[6]G. Cocconi, Phys. Rev. **111**, 1699 (1958); see also Ref. 10.
[7]M. Basile *et al.*, Nuovo Cimento **73A**, 329 (1983).

[8]T. T. Chou and Chen Ning Yang, Phys. Lett. **128B**, 457 (1983).
[9]E. Fermi, Prog. Theor. Phys. (Kyoto) **5**, 570 (1950).
[10]T. T. Chou and Chen Ning Yang, Phys. Lett. **116B**, 301 (1982).
[11]K. Alpgard *et al.*, Phys. Lett. **123B**, 361 (1983).
[12]J. G. Rushbrooke, in *Proceedings of the Fourteenth International Symposium on Multiparticle Dynamics, Lake Tahoe, 1983,* edited by P. M. Yager and J. F. Gunion (World Scientific, Singapore, 1984).
[13]J. G. Rushbrooke, in *Proceedings of the DPF Workshop on $\bar{p}p$ Options for the Super Collider, Chicago, 1984,* edited by J. E. Pilcher and A. R. White (Physics Department, University of Chicago, Chicago, 1984).
[14]Non-single-diffractive charged multiplicity at ISR and SPS Collider energies has been given in A. Breakstone *et al.*, Phys. Rev. D **30**, 528 (1984); G. J. Alner *et al.*, Phys. Lett. **138B**, 304 (1984). We use the formula $\bar{n}_{\rm ch}=2.88-0.0867\ln s+0.171\ln^2 s$ for extrapolation to higher energies.
[15]H. W. Lewis, J. R. Oppenheimer, and S. A. Wouthuysen, Phys. Rev. **73**, 127 (1948); S. Z. Belen'kji and L. D. Landau, Nuovo Cimento Suppl. **3**, 15 (1956); K. Niu, Nuovo Cimento **10**, 994 (1958); D. Amati, A. Stanghellini, and S. Fubini, *ibid.* **26**, 896 (1962); L. Van Hove, Rev. Mod. Phys. **36**, 655 (1964); R. Hagedorn, Nuovo Cimento Suppl. **3**, 147 (1965); J. Benecke, T. T. Chou, C. N. Yang, and E. Yen, Phys. Rev. **188**, 2159 (1969); R. P. Feynman, Phys. Rev. Lett. **23**, 1415 (1969); S. Barshay, Phys. Lett. **42B**, 457 (1972); C. M. G. Lattes, Y. Fujimoto, and S. Hasagawa, Phys. Rep. **65**, 151 (1980). See also Refs. 4, 6, and 9, and L. Stodolsky, Phys. Rev. Lett. **28**, 60 (1972); A. Buras and Z. Koba, Lett. Nuovo Cimento **6**, 629 (1973); J. Benecke, A. Białas, and E. de Groot, Phys. Lett. **57B**, 447 (1975); J. Benecke, A. Białas, and S. Pokorski, Nucl. Phys. **B110**, 488 (1976). A partial list of theoretical papers on multiparticle productions can be found in *Multiparticle Production at High Energies,* edited by T. Kobayashi and I. Ohba (Physical Society of Japan, Tokyo, 1978).
[16]T. T. Chou and Chen Ning Yang, Report No. UGA-HE-52 or ITP-SB-85-32 (unpublished).